JAERI - M
84-060

DIFFUSION PHENOMENA OF FLUORINE AND CATIONS IN MOLTEN Li_2BeF_4, $LiBeF_3$ AND $NaBeF_3$

March 1984

Hideo OHNO

日本原子力研究所
Japan Atomic Energy Research Institute

JAERI-M レポートは，日本原子力研究所が不定期に公刊している研究報告書です。

入手の問合わせは，日本原子力研究所技術情報部情報資料課（〒319—11 茨城県那珂郡東海村）あて，お申しこしください。なお，このほかに財団法人原子力弘済会資料センター（〒319—11 茨城県那珂郡東海村日本原子力研究所内）で複写による実費頒布をおこなっております。

JAERI-M reports are issued irregularly.

Inquiries about availabiljty of the reports should be addressed to Information Section, Division of Technical Information, Japan Atomic Energy Research Institute, Tokai-mura, Naka-gun, Ibaraki-ken 319—11, Japan.

編集兼発行　日本原子力研究所

印　　刷　㈱原子力資料サービス

JAERI-M 84-060

DIFFUSION PHENOMENA OF FLUORINE AND CATIONS IN MOLTEN Li_2BeF_4, $LiBeF_3$ AND $NaBeF_3$

Hideo OHNO

Department of Fuels and Materials Research,
Tokai Research Establishment, JAERI

(Received February 7, 1984)

Self-diffusion coefficients of fluorine and cations in molten $LiF-BeF_2$ and $NaF-BeF_2$ systems were summarized by the capillary reservoir technique. The diffusion coefficients and the activation energies of cations in these molten salts follow a similar behavior with those of cations in molten alkali halides. On the other hand, self-diffusion of fluorine have unusually high diffusion coefficients and activation energies. The characteristic diffusion phenomena of fluorine in these molten alkali fluoroberyllates are very similar to those of oxygen in molten $CaO-SiO_2$ and $CaO-SiO_2-Al_2O_3$ slag. The dynamical behavior of Li and F in molten Li_2BeF_4 was also analyzed by NMR technique. According to both these experiments, most probable mechanism of characteristic diffusion of fluorine in these molten systems could be dissociation of F atom from complex anion and long distance diffusion.

Keywords: Molten Salt, Alkali Fluoroberyllate, Alkaline-earth Silicates, Self-diffusion Coefficient, Nuclear Magnetic Resonance, Flibe, X-ray Diffraction Analysis, Fluorine, Cations

JAERI－M 84－060

溶融 Li_2BeF_4，$LiBeF_3$ および $NaBeF_3$ 中における フッ素およびカチオンの拡散現象

日本原子力研究所東海研究所燃料工学部
大野　英雄

（1984年2月7日受理）

本報告は過去10年近くにわたり行ってきた，溶融 Li_2BeF_4，$LiBeF_3$ および $NaBeF_3$ 中のフッ素ならびにカチオンの自己拡散現象について総合的にまとめたものである。これら溶融塩中におけるカチオンの自己拡散係数は，活性化エネルギーも小さく，典型的なアルカリハライド液体と同様な挙動を示す。一方，これら溶融塩中のフッ素の挙動は，活性化エネルギーも大きく，高温で大きな自己拡散係数をもち，溶融アルカリ土類珪酸塩中の酸素と同様な挙動を示す。核磁気共鳴の解析結果と併わせ考えると，跳躍拡散模型（一つの錯イオンからフッ素が解離し，液中を拡散して，他の錯イオンのF空孔にとらえられる）が，この異常なフッ素の自己拡散現象を説明し得る最も可能性の高い模型のように思われる。

Contents

目　　次

1. Introduction

It has been reported that the alkali fluoroberyllate melt systems, $RF-BeF_2$ (R=Li, Na and K) are quite similar to the alkaline-earth silicate melt systems, $R'O-SiO_2$ (R'=Mg, Ca and Ba). Especially, the phase diagram of $MgO-SiO_2$ scaled down by the relation $(t°C+273°C)/2.88+273$ fit most of the diagram of $LiF-BeF_2$ as shown in Fig.1[1]. It was also recently found that the physical properties, such as viscosity, electrical conductivity, and molar volume, depend on simple quantitative relationships between molten alkali fluoroberyllate systems and molten alkaline-earth silicate systems[2]. Some typical results of molar volume and viscosity are shown in Figs.2,3,4, and 5[2]. This is due to the reason that the ratio of ionic radius constituing both alkali fluoroberyllates and alkaline-earth silicate systems have similar values as shown in Table 1.

The results indicate that the statistical and dynamical properties of constituent ions in these molten states have also similar behavior.

Cantor et al.[3] showed in their viscosity study of molten $LiF-BeF_2$ system that the viscosity decreases rapidly with an increase of LiF concentration, due to breaking of the fluorine bridges in a three-dimensional network of Be-F bonds, and estimated that the melt might lose its network charactor for a BeF_2 content smaller than 65mol %.

We have already reported the self-diffusion coefficients and their temperature dependence for F and Li in molten Li_2BeF_4

and $LiBeF_3$ and for F and Na in molten $NaBeF_3$ by the capillary reservoir technique[4]-[8], X-ray diffraction analysis of molten Na_2BeF_4 and $NaBeF_3$[9] and nuclear spin relaxation of ^7Li and ^{19}F in solid and molten Li_2BeF_4[10]. In this report, all these data are summarized and compared with those in molten alkaline-earth silicates.

2. Experimentals

The method of measurements of self-diffusion coefficients was described in detail elsewhere[4]-[8]. The procedure of the experiment was carried out by the capillary reservoir technique.

2.1 Preparation of radioactive or stable tracer

The fluorine radioactive F-18 was prepared using JRR-2(Japan Research Reactor -2). Highly purified Li_2CO_3 was used as a target materials and the following reactions occured to produce ^{18}F.

$$^{6}_{3}Li(n,\alpha)^{3}_{1}T \quad \text{and} \quad ^{16}_{8}O(T,n)^{18}_{9}F \qquad ---(1)$$

After irradiation, Li_2CO_3 powder was treated with aqueous hydrogen fluorine in a platinum crucible to produce the labelled $Li^{18}F$ deposit. The observed half-life time of ^{18}F was 111 min. as shown in Fig.6.

On the other hand, the stable ^6Li was prepared using Li_2CO_3 powder which has a $^6Li/^7Li$ abundance ratio of 19 and then Li_2CO_3

and $LiBeF_3$ and for F and Na in molten $NaBeF_3$ by the capillary reservoir technique[4]-[8], X-ray diffraction analysis of molten Na_2BeF_4 and $NaBeF_3$[9] and nuclear spin relaxation of ^7Li and ^{19}F in solid and molten Li_2BeF_4[10]. In this report, all these data are summarized and compared with those in molten alkaline-earth silicates.

2. Experimentals

The method of measurements of self-diffusion coefficients was described in detail elsewhere[4]-[8]. The procedure of the experiment was carried out by the capillary reservoir technique.

2.1 Preparation of radioactive or stable tracer

The fluorine radioactive F-18 was prepared using JRR-2(Japan Research Reactor -2). Highly purified Li_2CO_3 was used as a target materials and the following reactions occured to produce ^{18}F.

$$^{6}_{3}Li(n,\alpha)^{3}_{1}T \quad \text{and} \quad ^{16}_{8}O(T,n)^{18}_{9}F \qquad ---(1)$$

After irradiation, Li_2CO_3 powder was treated with aqueous hydrogen fluorine in a platinum crucible to produce the labelled $Li^{18}F$ deposit. The observed half-life time of ^{18}F was 111 min. as shown in Fig.6.

On the other hand, the stable ^6Li was prepared using Li_2CO_3 powder which has a $^6Li/^7Li$ abundance ratio of 19 and then Li_2CO_3

was treated with aqueous hydrogen fluorine in the same way as above mentioned. ^{24}Na was made from NaF powder irradiated by thermal neutron for 1 min. in JRR-2.

2.2 Preparation of Li_2BeF_4, $LiBeF_3$ and $NaBeF_3$

For the preparation of Li_2BeF_4, $LiBeF_3$ and $NaBeF_3$ in the diffusion cell, a mixture of BeF_2 and LiF or NaF was melted in a platinum container, treated with a $HF+H_2$ mixture at about 600°C and then purged with He. The chemicals used were as follows: LiF and NaF prepared by Merck Co.(Germany), granulation of single crystal(1-4mm); BeF_2 prepared by Rare Metallic Co.(Japan) known impurities(in ppm):K+Na,600;Ca,10;Al,20;Cr,30;Fe,10;Ni,10 .

2.3 Apparatus and procedure

A schematic diagrams of the apparatus is shown in Fig.7. In this work some devices were adopted to avoid solidification of the melted tracer mixture in the capillaries before each diffusion run. After the tracer salt(C) in the Pt crucible(D) and non-tracer salt(E) in the Ni crucible(F) were melted under He atmosphere, the movable Ni rod with the capillaries was lowered into the Pt crucible. The capillaries were filled with the molten tracer salt by dipping their mouths into the salt under a vacuum and then feeding He gas slowly back in the apparatus. The capillaries were raised out of the molten tracer salt by means of the moval Ni rod and then submerged in the molten non-tracer salt after turning the stainless steel flange(I).

The capillaries which were 1mm inner diameter and 30-40mm length were made of Ni. The duration of diffusion run was in the range of 20-120 minutes. The maximum difference in temperature between the top and the bottom of the capillary was about 0.5°C.

After the diffusion run, the capillaries were lifted from the non-tracer salt and then removed. After cleaning the capillaries, those were cut by a saw at intervals of about 2mm. The concentration profiles of tracer ^{18}F and ^{24}Na or ^{6}Li in the capillaries were measured with γ-ray spectrometer or ion micro mass analyser(HITACHI IMA-SS), respectively.

2.4 Nuclear magnetic resonance

Spin-lattice relaxation time T_1 was measured by pulse spectrometer controlled by a micro-processer. For T_1 values less than 0.1sec "180°-τ-90°" pulse technique was applied and the longer T_1 was measured by "(n·90°)-τ-90°" pulse technique. The 90° pulse length was about 15μs. For magnetization $M_z(\tau)$ the intensity of free induction decay(FID) signal following second 90° pulse were measured as a function of τ. The absolute $M_z(\tau)$ decay obeyed exponential law in all samples. In order to improve signal to noise ratio a digitalized signal average were utilized. In all experiments a frequency of 10MHz or 20MHz was employed. Each sample was sealed in quartz sample tube with the length of 4cm and the diameter of 1cm. Temperature of the specimens was controlled up to 630°C with accuracy of ±2°C in an electrical furnace which was mounted between pole pieces of magnet. Temperature was

measured by an Pt-Pt(13%Rh) thermocouple attached to the sample tube

T_1 for ^{7}Li and ^{19}F has been determined using the relation $I=I_0(1-\exp(-\tau/T_1))$ for relatively long T_1 ($T_1>0.1$sec) or $I=I_0(1-2\exp(-\tau/T_1))$ for relatively short T_1 ($T_1<0.1$sec).

3. Results and discussion

Typical concentration profiles of ^{18}F and ^{6}Li in capillaries are shown in Figs.8 and 9. The salt was not contained within a few mm from the capillary mouth due to the volume contraction of the salt.

The diffusion coefficient D was calculated by applying the following equation to the observed concentration profiles,

$$C_x=C_0\mathrm{erf}(x/(Dt)^{1/2}), \qquad ---(2)$$

where C_0 is the initial concentration of the tracer and C_x the concentration of the tracer at distance x from the boundary after diffusion time t. Figs.10,11,12 and 13 show the observed raw data of diffusion coefficient of Li,Na,and F in molten Li_2BeF_4, $LiBeF_3$ and $NaBeF_3$. The observed data of diffusion coefficients of constituent ions in molten LiF-NaF-KF eutectic mixture(FLINAK) is also shown in Fig.14.

The diffusion coefficients are written in the form

$$D=D_0\exp(-E/RT), \qquad ---(3)$$

where E is the activation energy, R the gas constant and T the absolute temperature. The results as shown in Table 2 and Fig.15

measured by an Pt-Pt(13%Rh) thermocouple attached to the sample tube

T_1 for ^{7}Li and ^{19}F has been determined using the relation $I=I_0(1-\exp(-\tau/T_1))$ for relatively long T_1(T_1>0.1sec) or $I=I_0(1-2\exp(-\tau/T_1))$ for relatively short T_1(T_1<0.1sec).

3. Results and discussion

Typical concentration profiles of ^{18}F and ^{6}Li in capillaries are shown in Figs.8 and 9. The salt was not contained within a few mm from the capillary mouth due to the volume contraction of the salt.

The diffusion coefficient D was calculated by applying the following equation to the observed concentration profiles,

$$C_x=C_0\mathrm{erf}(x/(Dt)^{1/2}), \qquad ---(2)$$

where C_0 is the initial concentration of the tracer and C_x the concentration of the tracer at distance x from the boundary after diffusion time t. Figs.10,11,12 and 13 show the observed raw data of diffusion coefficient of Li,Na,and F in molten Li_2BeF_4, $LiBeF_3$ and $NaBeF_3$. The observed data of diffusion coefficients of constituent ions in molten LiF-NaF-KF eutectic mixture(FLINAK) is also shown in Fig.14.

The diffusion coefficients are written in the form

$$D=D_0\exp(-E/RT), \qquad ---(3)$$

where E is the activation energy, R the gas constant and T the absolute temperature. The results as shown in Table 2 and Fig.15

were obtained by a least squares analysis from all experimental data.

Figs.16 and 17 show the results of self-diffusion coefficients in these molten alkali fluoro-beryllates compared with those of cations and anions in molten alkali halides and molten silicates under the reduced temperature scale, T/T_m, where T_m is the melting point. The diffusion coefficients and the activation energies of cations in molten Li_2BeF_4,$LiBeF_3$ and $NaBeF_3$ follow a similar pattern to those of cations in molten alkali halides. On the other hand, self-diffusion of fluorine in these molten alkali fluoro-beryllates have unusually high diffusion coefficinets and activation energies. The activation energies for self-diffusion coefficients of fluorine were larger than those for electrical conductivities[11] and viscosity coefficients[3].

It was reported by the analysis of X-ray diffraction[9][12] and the Raman spectrum measurements[13] that independent anion exist, such as BeF_4^{2-} and $Be_2F_7^{3-}$ in molten Li_2BeF_4,$LiBeF_3$ and $NaBeF_3$. Figs.18 and 19 show the radial distribution functions of molten Na_2BeF_4 and $NaBeF_3$ by X-ray diffraction analysis[9]. In molten Na_2BeF_4, the observewd coordination number of the nearest neighbor Be-F($n_{Be/F}$) and F-F($n_{F/F}$) pairs were 4.0 and 3.0,respectively. This suggests that BeF_4 tetrahedra exist mainly in an isolated form with four unshared F^- corners, monomeric BeF_4^{2-}, in molten Na_2BeF_4. As the BeF_2 concentration increases, the polymerization process proceeds and pure BeF_2 forms a three-dimensional network structure of BeF_4 tetrahedra. $NaBeF_3$ is the intermediate

phase between these composition extremes. In molten $NaBeF_3$ the observed coordination number $n_{Be/F}$ and $n_{F/F}$ were 3.8 and 3.5, respectively. The calculated average $n_{F/F}$ of chain anions such as $Be_2F_7^{3-}$, $Be_3F_{10}^{4-}$, $Be_4F_{13}^{5-}$ and $(BeF_3)_\infty^{\infty-}$ are 3.4, 3.6, 3.7 and 4.0, respecively. On the other hand, the value of $n_{F/F}$ for closed-ring anions is always 4.0. Therefore, the possibility of small-chain anions such as $Be_2F_7^{3-}$ and $Be_3F_{10}^{4-}$ is considered to be large in molten $NaBeF_3$.

The fact that the magnitude of the diffusion coefficient measured in this work is extraordinary large can not be explained solely by mass transfer due to migration of the large fluoroberyllate anions.

Possible explanation for the large value of the fluorine diffusion coefficient could be the exchange of fluorine atoms between neighbouring beryllate units including the rotation of beryllate anions, or the fluorine diffusion by means of neutral ion pair, such as LiF, diffusion mechanism. The exchange mechanism involves the breaking of Be-F bonds and some steric difficulties with anion rotation, which can account for a high energy of activation for fluorine diffusion. In ion pair diffusion, on the other hand, the movement of fluorine with lithium involves breaking of Be-F bonds, because the content of free fluorine atoms in the melt seems small. This mecanism can also have a high activation energy.

Fig.20 shows the temperature dependence of spin-lattice relaxation time T_1 of ^{19}F and ^{7}Li in molten Li_2BeF_4[10]. T_1 of

^{19}F had maximum and T_1 at frequency of 20MHz was longer than that at frequency of 10MH at temperatures below T_1 minimum. However, both values of T_1 approached to the same at temperatures above T_1 minimum. T_1 of ^{7}Li had also minimum and the minimum temperature of ^{7}Li was a little higher than that of ^{19}F.

The magnetic impurities such as Ni^{2+} and Fe^{2+} in the sample will have important effect upon the relaxation time and resonance absorption spectra. The concentration of magnetic impurity was estimated by the analysis of magnetic susceptibility measured at temperatures below 4.2K. The concentration of magnetic impurity used in the measurements of NMR was about 2.9ppm calculated in terms of Fe^{2+} ion.

Fig.21 shows the resonance absorption spectra of ^{19}F and ^{7}Li in solid and molten Li_2BeF_4(10). The frequency was 10MHz. The remarkable result was the line width of resonance absorption spectrum of ^{19}F at 435°C(solid) is nearly equal to that at 550°C (liquid).

As there is mainly BeF_4^{2-} and Li^{+} ions in molten Li_2BeF_4, the following relaxation mechanisms will be considered as the relaxation of ^{19}F.

(1) Rotation of BeF_4^{2-} ion.

(2) Migration of BeF_4^{2-} ion.

(3) Dissociation of F atom from BeF_4^{2-} ion and diffusion of fluorine.

The contribution of these three mechanisms to T_1 are shown in Ref(10) precisely and the essential equations and results will

be presented in this paper.

(1) Relaxation due to the rotation of BeF_4^{2-} ion

There are two models, diffusion model and kinetic model. In diffusion model, the relaxation time of rotation τ_2 is much shorter than periodic time of rotation T_0 ($\tau_2 \ll T_0$) and T_1 is expressed by the folowing equation,

$$(1/T_1)_{rot.diff}=(2/5)(\gamma-1)\gamma_F^4 \hbar^2 r_{F-F}^{-6} I_F(I_F+1) \times(\tau_2/(1+\omega^2\tau_2^2)+4\tau_2/(1+4\omega^2\tau_2^2)). \quad ---(4)$$

On the other hand, T_1 in kinetic model($\tau_2 > T_0$) is expressed by the following equation,

$$(1/T_1)_{rot.kin}=(1/5)(1/T_1)_{rot.diff}. \quad ---(5)$$

In these equations, I_F is the quantum number of F nuclear spin(=1/2), γ the number of F atoms in BeF_4^{2-} ion(=4), γ_F the gyromagnetic ratio of F nuclei and r_{F-F} the atomic distance of F-F pair.

The diffusion coefficient D' of rotation of complex ion is expressed by Stokes relation with viscosity η.

$$D'=kT/8\pi a^3\eta . \quad ---(6)$$

The relaxation time τ_2 will be calculated using the relation $\tau_2=(6D')^{-1}$ and the observed viscosity $\eta=5.94\times10^{-4}\exp(38.4/RT)$ poise[3]. τ_2 at 530°C was roughly estimated to be 1.7×10^{-10}s.

On the other hand, eq.(4) is expressed using parameter $r_{F-F}=2.56$A as follows.

$$(1/T_1)_{rot}=1.7\times10^9(\tau_2/(1+\omega^2\tau_2^2) + 4\tau_2/(1+4\omega^2\tau_2^2))s^{-1}. \quad (7)$$

This equation has maximum at $\tau_2=0.64$. The estimated relaxation time by Stokes relation $\tau_2=1.7\times10^{-10}$s show $\omega\tau_2=1.02\times10^{-2}$ which is much smaller than the observed value $(1/T_1)_{exp}=200s^{-1}$. Then the contribution of rotation to T_1 will be small.

(2) Relaxation due to the migration of BeF_4^{2-} ion.

T_1 due to the migration of complex ion will be expressed by

$$(1/T_1)_{diff}=3/2\ \gamma^4\hbar^2 I(I+1)(8\pi/15J(\omega)+32\pi/15J(2\omega))\text{--}(8)$$

and

$$J(\omega)=(N/dD)\int_0^\infty (J_{3/2}(u))^2\ udu/(u^4+\omega^2\tau^2),\text{---}(9)$$

where D is the diffusion coefficient of migration of complex ion, N the spin density, d the diameter of complex ion and $J_{3/2}$ Bessel function. The integration in eq.(9) has maximum value 0.133 at $\omega\tau=0$ and decreases monotonously. Then $(1/T_1)_{diff}$ has no maximum.

The diffusion coefficient D of migration of complex ion is roughly estimated by Stokes relation $D=kT/6\pi a\eta$ and D is $1\times10^{-10}m^2/s$ at 530°C. Then using $N=7\times10^{30}/m^3$ and $D=1\times10^{-10}m^2/s$ (530°C), the contribution of migration of BeF_4^{2-} ion to T_1 is estimated to be $(1/T_1)_{diff}=0.3$, which is also much smaller than the observed value.

(3) Dissociation of F atom from BeF_4^{2-} ion and diffusion of fluorine

The behavior of T_1 is attributed to the dissociation of

F from complex ions and the long distance diffusion of F ions in the liquid by the following reasons.

In exchange model as shown in Fig.22 of fluorine atoms between neighbouring beryllate units including rotation of beryllate anion, the diffusion distance with one step will be at most 6Å. Using the relation $D=\langle a^2 \rangle / 6\tau$ and the obserevd diffusion coefficient $D=2\times10^{-9} m^2/s$ at 530°C, the estimated correlation time τ is 2×10^{-11}s which is much smaller than the observed $\tau=3\times10^{-9}$s and is comparable with that of the rotation of the molecule. This is not reasonable.

On the other hand, in dissociation and long distance diffusion model of fluorine, the relaxation time will be expressed by the following equation[14].

$$1/T_1=8\pi/15\cdot\gamma^4\hbar I(I+1)N/a^3\left[\tau/(2(1+(\omega\tau/2)^2))+\tau/(1+\omega^2\tau^2)\right] \quad --(10)$$

Equation (10) has maximum at $\omega\tau=1.41$ ($\tau=2.25\times10^{-8}$s at $\omega=6.28\times10^7 s^{-1}$) and we get $(1/T_1)_{max}=50$, which is much larger than the former two relaxation mechanisms. Then root mean square (RMS) distance $\sqrt{\langle \ell^2 \rangle}$ of one step of fluorine diffusion, which is the distance between dissociation of F from a complex ion, diffusion in the liquid and trap at F vacancy of another complex ion, is roughly estimated by relation $\langle \ell^2 \rangle = 6\tau D$. At 530°C, the observed value of τ and D were 2.25×10^{-8}s and $2\times10^{-9} m^2/s$, respectively and $\sqrt{\langle \ell^2 \rangle} \simeq 100$Å was obtained.

The results of NMR indicate that the dissociation of F from complex ions and the long distance diffusion of F ions has largest contribution to the diffusion in molten Li_2BeF_4

and T_1 of this mechanism is in good agreement with the experimental value. The solid curves in Fig.23 are the theoretical one with

$$1/\tau=2\times10^{15}\ \exp(-103.7/RT), \quad ---(11)$$

and

$$1/T_1=S[\tau/(1+\omega^2\tau^2) + 4\tau/(1+4\omega^2\tau^2)]. \quad ---(12)$$

S was determined to fit the theoretical curve to the observed one at 640°C and $\omega=2\pi\times10^7 s^{-1}$. The theoretical equation indicates good agreement with temperature and frequency dependency of the observed T_1. The activation energy 103.7KJ/mol is also in good agreement with that of self-diffusion of fluorine with tracer method 128KJ/mol as shown in Table 2.

4. Conclusions

(1) Characteristic diffusion of fluorine in molten alkali fluoroberyllates could be the diffusion mechanism with dissociation of F from complex anion and long distance diffusion.

(2) The results of self-diffusion of fluorine in molten Li_2BeF_4, $LiBeF_3$ and $NaBeF_3$ are qualitatively similar to those of oxygen in molten $CaO-SiO_2$ and $CaO-SiO_2-Al_2O_3$ slag[15][16]. X-ray diffraction analysis of molten $NaBeF_3$[9] and $CaSiO_3$[17] also indicates the similarity of molten structure as shown in Fig.24. Then the research for molten alkali fluoroberyllates will contribute to the analysis of statistical and dynamical behaviours of constituent ions in molten alkali-

and T_1 of this mechanism is in good agreement with the experimental value. The solid curves in Fig.23 are the theoretical one with

$$1/\tau=2\times10^{15}\ \exp(-103.7/RT), \quad ---(11)$$

and

$$1/T_1=S[\tau/(1+\omega^2\tau^2)\ +\ 4\tau/(1+4\omega^2\tau^2)]. \quad ---(12)$$

S was determined to fit the theoretical curve to the observed one at 640°C and $\omega=2\pi\times10^7 s^{-1}$. The theoretical equation indicates good agreement with temperature and frequency dependency of the observed T_1. The activation energy 103.7KJ/mol is also in good agreement with that of self-diffusion of fluorine with tracer method 128KJ/mol as shown in Table 2.

4. Conclusions

(1) Characteristic diffusion of fluorine in molten alkali fluoroberyllates could be the diffusion mechanism with dissociation of F from complex anion and long distance diffusion.

(2) The results of self-diffusion of fluorine in molten Li_2BeF_4, $LiBeF_3$ and $NaBeF_3$ are qualitatively similar to those of oxygen in molten $CaO-SiO_2$ and $CaO-SiO_2-Al_2O_3$ slag[15][16]. X-ray diffraction analysis of molten $NaBeF_3$[9] and $CaSiO_3$[17] also indicates the similarity of molten structure as shown in Fig.24. Then the research for molten alkali fluoroberyllates will contribute to the analysis of statistical and dynamical behaviours of constituent ions in molten alkali-

earth silicates which is relatively difficult because of high temperature.

Acknowledgement

The author wishes to express his thank to Drs.K.Iwamoto, T.Kondo and J.Shimokawa for their interest in this work.

The author also wishes to thank to Prof.K.Furukawa(Tokai University), Drs.H.Katsuta and Y.Kato and Prof.T.Matsuo(Toyo University) for their helpful discussions.

earth silicates which is relatively difficult because of high temperature.

Acknowledgement

The author wishes to express his thank to Drs.K.Iwamoto, T.Kondo and J.Shimokawa for their interest in this work.

The author also wishes to thank to Prof.K.Furukawa(Tokai University), Drs.H.Katsuta and Y.Kato and Prof.T.Matsuo(Toyo University) for their helpful discussions.

References

(1) E.Thillo and H.A.Lehmann,Z.Anorg.Chem.,258,332(1949).

(2) K.Furukawa and H.Ohno,Trans.Japan Inst.Metal,19,553(1978).

(3) S.Cantor,W.T.Ward and T.Moyniham,J.Chem.Phys.,50,2874 (1969).

(4) H.Ohno,Y.Tsunawaki,N.Umesaki,K.Furukawa and N.Iwamoto, J.Japan Inst.Metals,41,391(1977)(in Japanese).

(5) T.Ohmichi,H.Ohno and K.Furukawa,J.Phys.Chem.,80,1628(1976).

(6) H.Ohno,K.Furukawa,Y.Tsunawaki,N.Umesaki and N.Iwamoto, J.Chem.Res.(S),1978,158.

(7) N.Iwamoto,Y.Tsunawaki,N.Umesaki,H.Ohno and K.Furukawa, J.Chem.Soc.,Faraday Trans.II, 75,1227(1979).

(8) Y.Tsunawaki,H.Ohno,H.Katsuta and K.Furukawa,Chem.Soc. Japan,1982,(6),956(in Japanese).

(9) N.Umesaki,N.Iwamoto,H.Ohno and K.Furukawa,J.Chem.Soc., Faraday Trans.1,78,2051(1982).

(10) T.Matsuo,H.Suzuki,H.Ohno and K.Furukawa, Chem.Soc.Japan, 1982,(6),892(in Japanese).

(11) G.D.Robbins and J.Braunstein in "Molten Salts:Characterization and Analysis", G.Mamantov,Ed.,Marcel Dekker,New York,N.Y.,1969,p.443.

(12) F.Vaslow and A.H.Narten,J.Chem.Phys.,59,4949(1973).

(13) A.S.Quist,J.B.Bates and G.E.Boyd,J.Phys.Chem.,76,78(1972).

(14) H.C.Torry,Phys.Rev.,92,962(1953).

(15) T.Saito,Y.Shiraishi,N.Nishiyama,K.Sorimachi and Y.Sawada, Proc.4th Japan-USSR Joint Symp.Phys.Chem.Metallurg.Processes,1973,p.53.

(16) P.J.Koros and T.B.King,Trans.AIME,224,299(1962).

(17) Y.Waseda,H.Suito and Y.Shiraishi,J.Japan Inst.Metals, 41,1068(1977)(in Japanese).

(18) K.Grjoheim and S.Zuka,Acta.Chem.Scand.,22,531(1968).

(19) J.O'M.Bockris and G.W.Hooper,Disc.Faraday Soc.,32,218(1961).

(20) D.Harari,F.Lantelme and M.Chemla,J.Chem.Phys.Physicochem. Biol.,66,1286(1969).

(21) J.O'M.Bockris,S.R.Richards and L.Nanis,J.Phys.Chem.,69, 1627(1965).

(22) T.Ejima,T.Yamamura and H.Hisamura,J.Japan Inst.Metals,41, 742(1977)(in Japanese).

(23) N.Umesaki,N.Iwamoto,Y.Tsunawaki,H.Ohno and K.Furukawa, J.Chem.Soc.,Faraday Trans.I,77,169(1981).

(24) Y.Guputa and T.B.King,Trans.AIME,239,1701(1967).

(25) R.F.Johnson,R.A.Stark and J.Taylor, Ironmaking and Steel-making,220(1974).

(26) H.Tower and J.Chipman,Trans.AIME,209,769(1957).

(27) T.Saitoh and K.Maruya,J.Japan Inst.Metals,21,778(1957) (in Japanese).

(28) C.Angel and W.Tomlinson,Trans.Faraday Soc.,61,2321(1965).

(29) Y.Shiraishi, private communication.

(30) A.Rahman,R.H.Fowler and A.H.Narten,J.Chem.Phys.,57,3010 (1971).

Table 1 Ratio of ionic radius constituing several alkaline-earth silicates and alkali fluoroberyllates.

	Ratio	
O^{2-}=1.40Å	1.03	1.36Å=F^-
$\frac{Mg^{2+}}{O^{2-}}$=0.46	1.05	0.44= $\frac{Li^+}{F^-}$
$\frac{Ca^{2+}}{O^{2-}}$=0.71	1.01	0.70= $\frac{Na^+}{F^-}$
$\frac{Ba^{2+}}{O^{2-}}$=0.29	0.99	0.98= $\frac{K^+}{F^-}$

Table 2 Summary of self-diffusion coefficients in molten Li_2BeF_4, $LiBeF_3$ and $NaBeF_3$.

$NaBeF_3$:

$$\begin{cases} D_{Na}=7.80\times10^{-7}\exp[(-40.2\pm5.6)\times10^3/RT] \\ \qquad\qquad (420\sim560°C) \\ D_F=4.93\times10^{-4}\exp[(-79.6\pm6.5)\times10^3/RT] \\ \qquad\qquad (440\sim600°C) \end{cases}$$

Li_2BeF_4 :

$$\begin{cases} D_{Li}=9.27\times10^{-7}\exp[(-32.5\pm8.4)\times10^3/RT] \\ \qquad\qquad (470\sim640°C) \\ D_F=6.61\times10^{-1}\exp[(-128.1\pm14.2)\times10^3/RT] \\ \qquad\qquad (510\sim650°C) \end{cases}$$

$LiBeF_3$:

$$\begin{cases} D_{Li}=1.12\times10^{-6}\exp[(-38.7\pm12.5)\times10^3/RT] \\ \qquad\qquad (440\sim560°C) \\ D_F=3.16\times10^{0}\exp[(-144.4\pm16.3)\times10^3/RT] \\ \qquad\qquad (450\sim670°C) \end{cases}$$

D : m^2 S^{-1} ; R : J mol^{-1} K^{-1} ; T : K

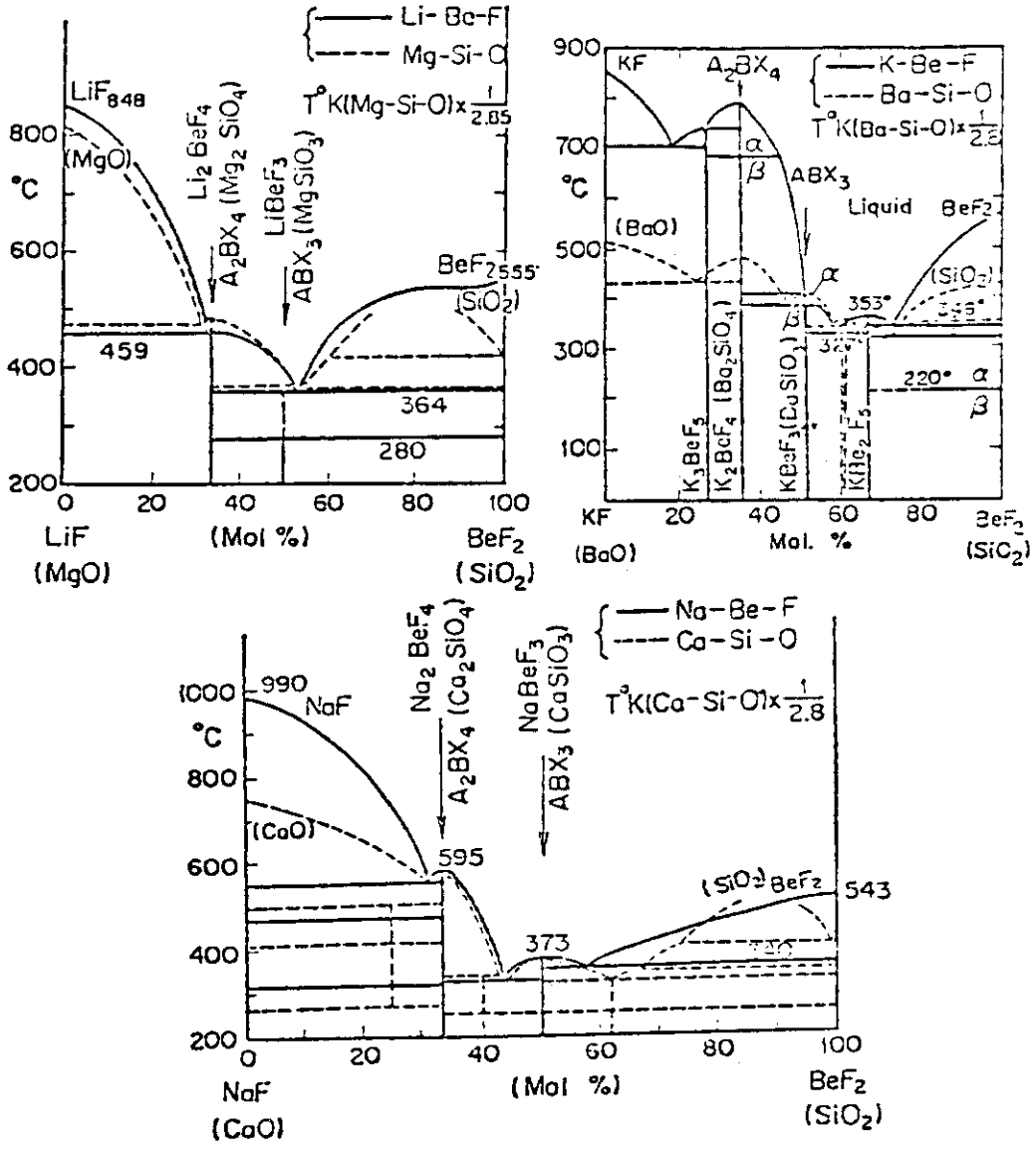

Fig.1 Comparison of phase diagrams of silicates and fluoroberyllates[1].

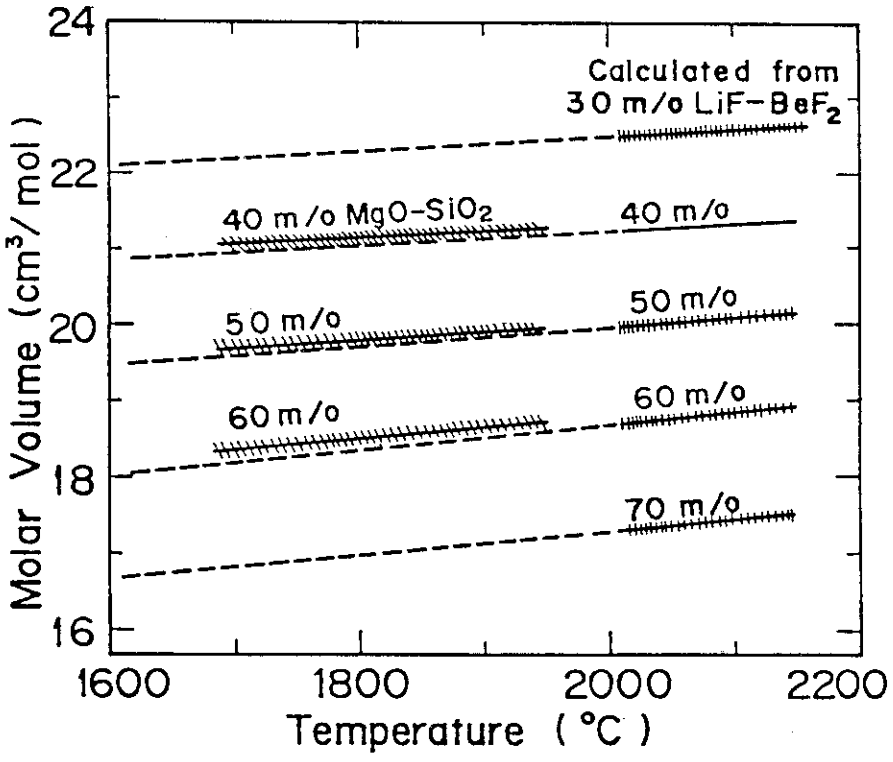

Fig.2 Comparison of molar volume of molten $MgO-SiO_2$ system between measured and calculated from those of molten $LiF-BeF_2$ system[2].

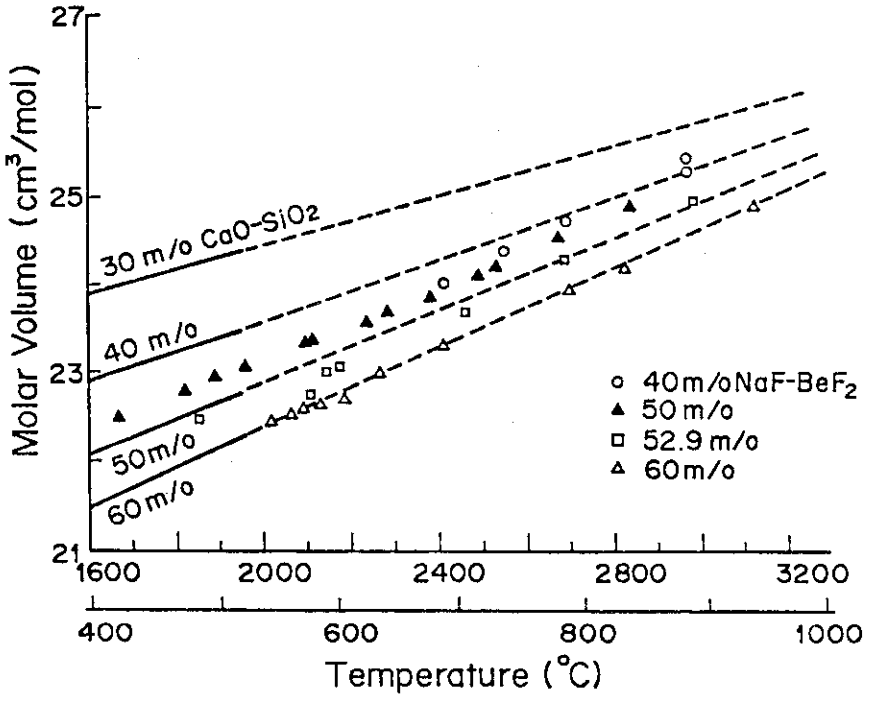

Fig.3 Comparison of molar volume of molten $CaO-SiO_2$ system between measured and calculated values from those of molten $NaF-BeF_2$ system.[2]

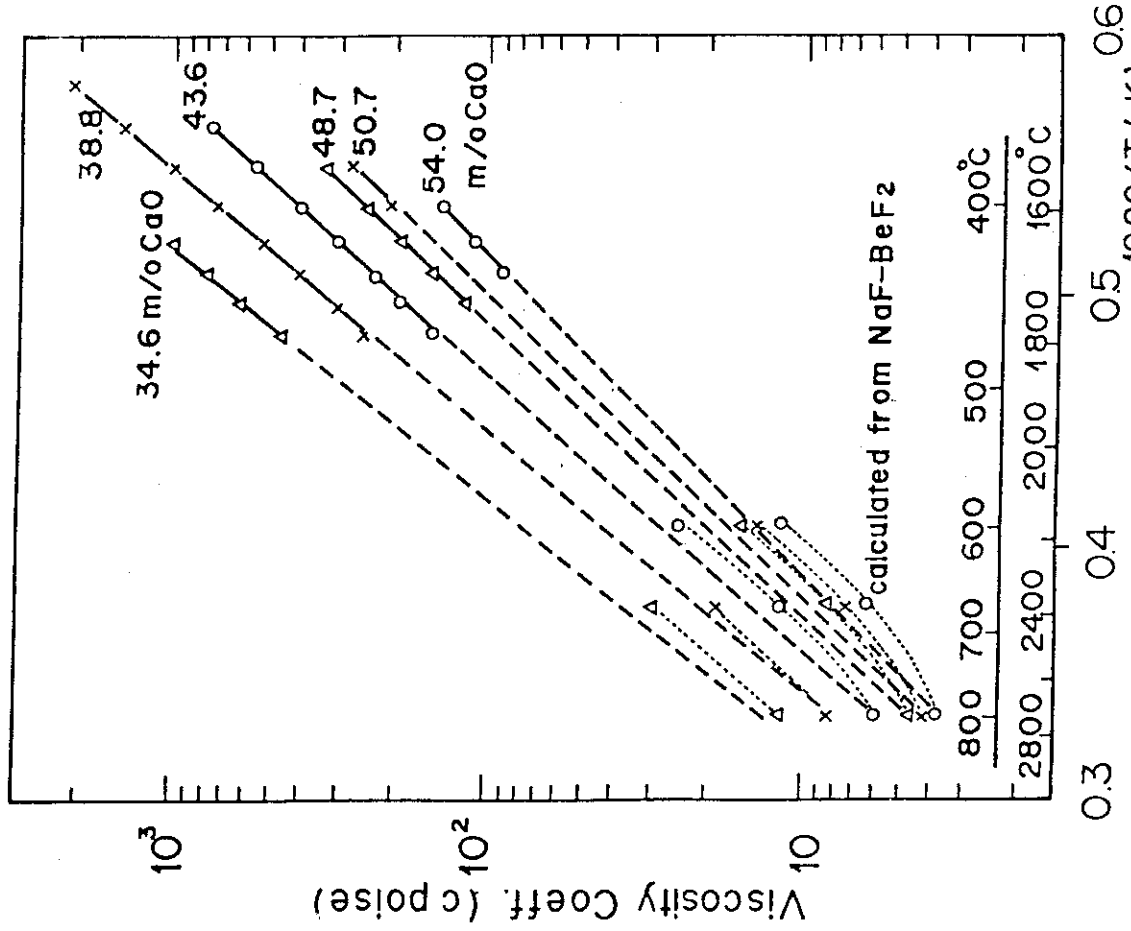

Fig.5 Comparisom of viscosity coefficients of molten $CaO-SiO_2$ and $NaF-BeF_2$ systems in the reduced temperature scale[2].

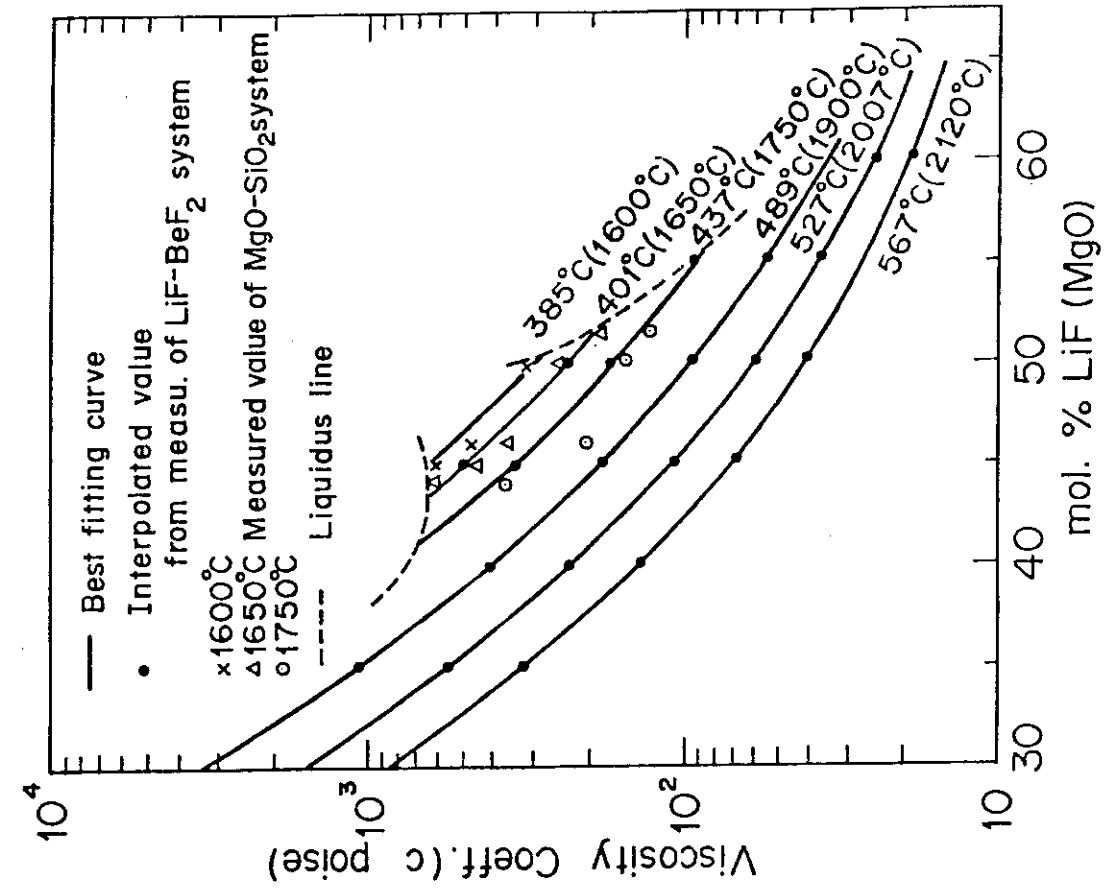

Fig.4 Comparison of viscosity coefficients of molten $MgO-SiO_2$ and $LiF-BeF_2$ systems in the reduced temperature scale.[2]

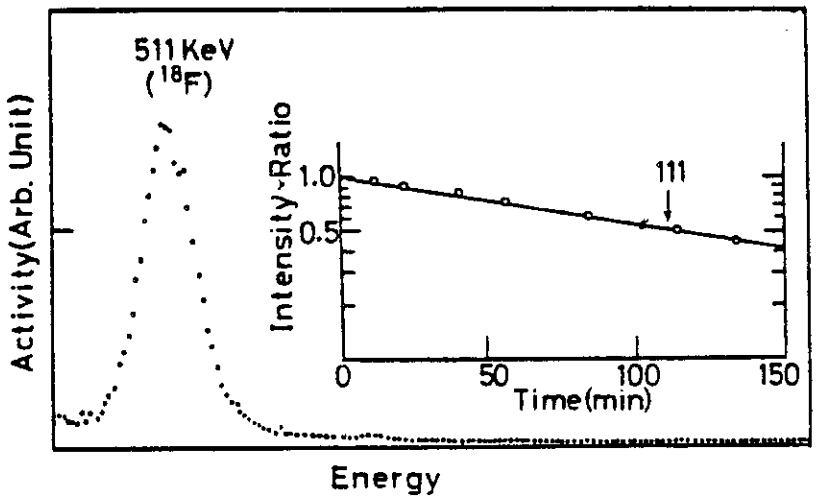

Fig.6 γ-ray spectrum and half-life time of ^{18}F(4).

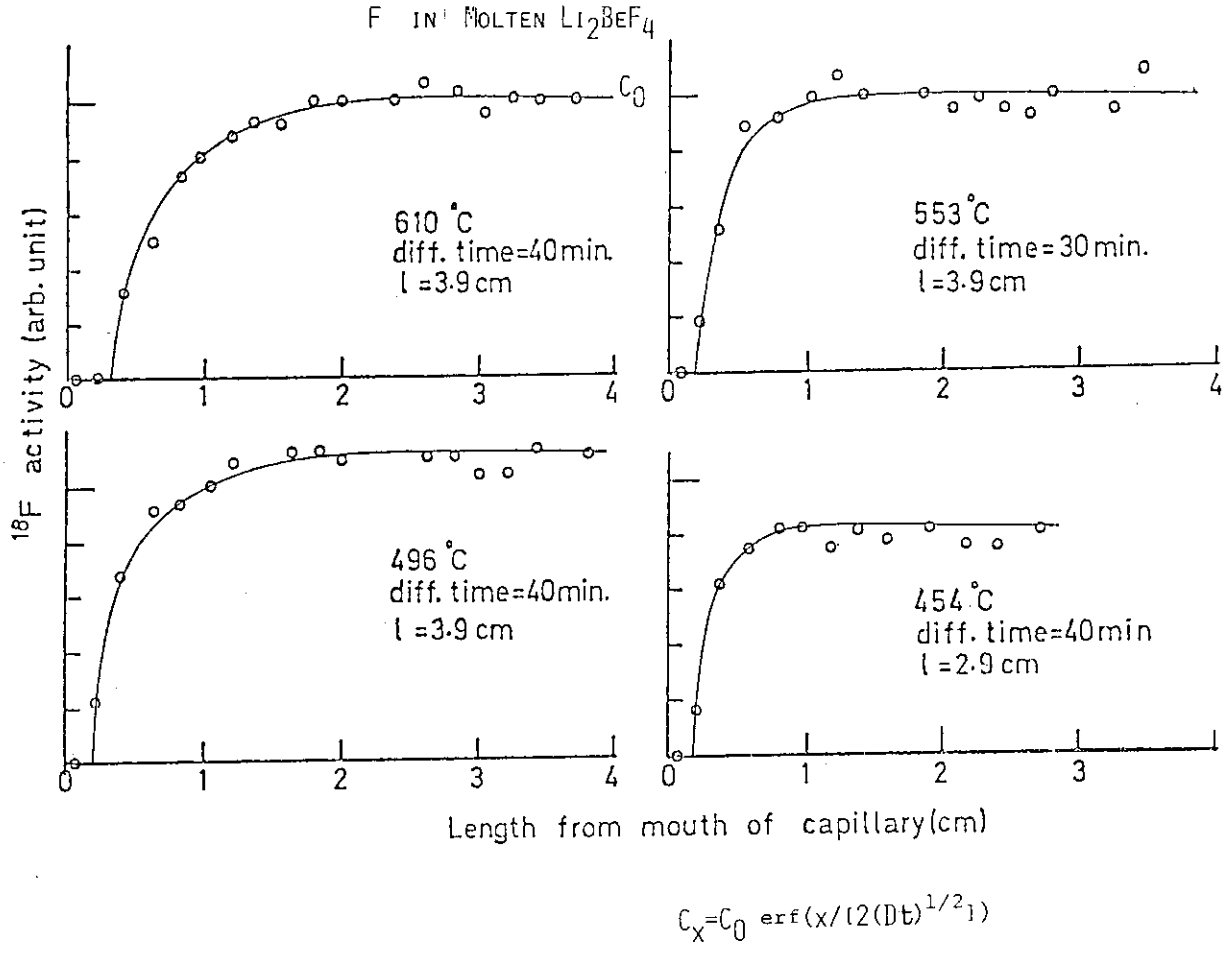

Fig.8 Distribution of ^{18}F in a capillary after a diffusion run.

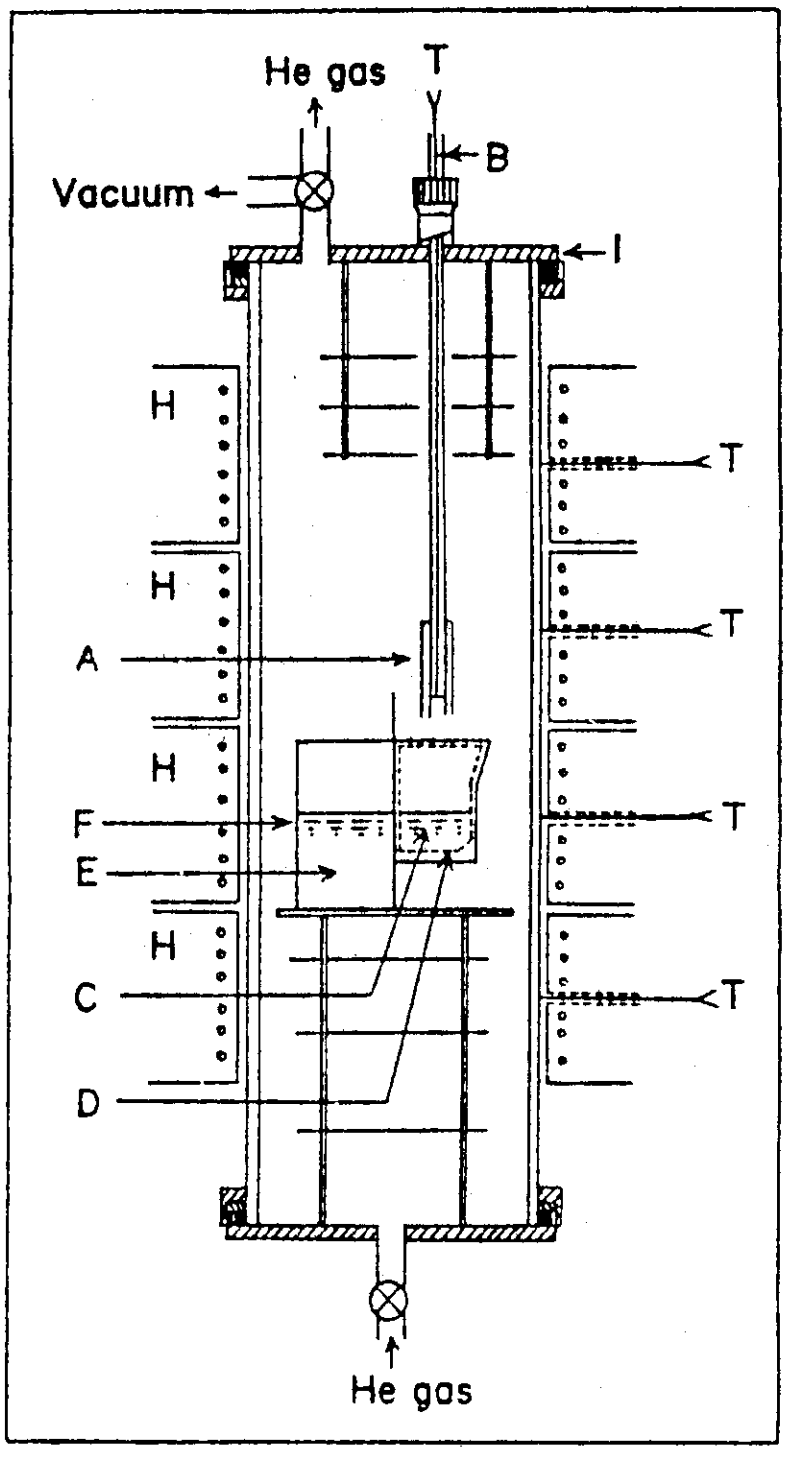

Fig.7 Apparatus for diffusion measurement.(7)

A:Ni capillary,B:Ni rod,C:Tracer salt,D:Pt crucible,E: Non-tracer salt,F:Ni crucible,H:Heater,I:Stainless steel flange,T:C.A.thermocouple.

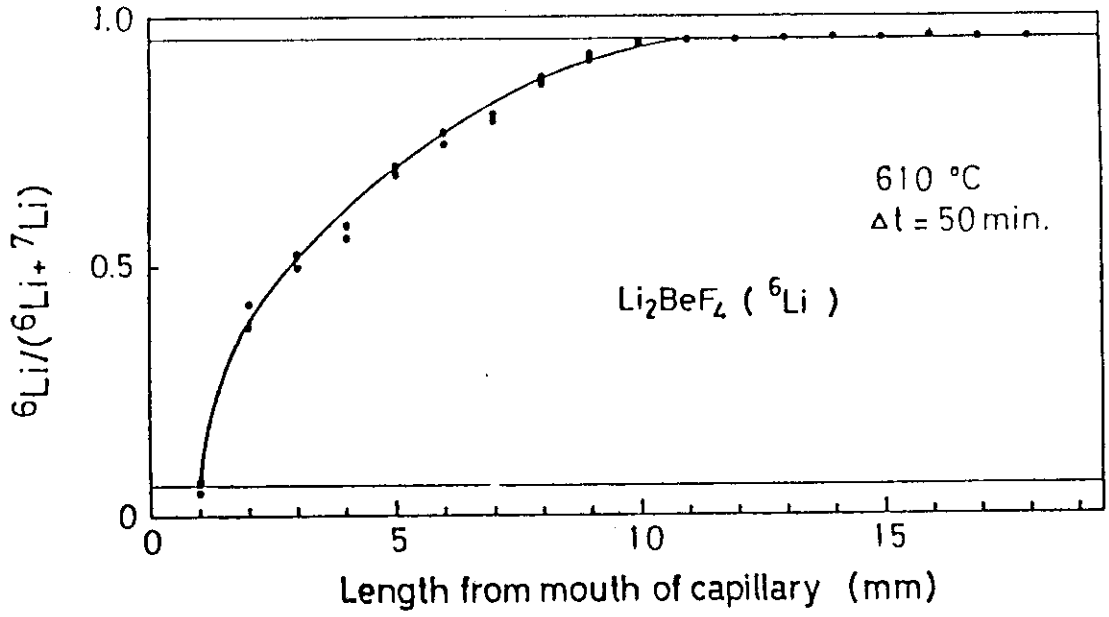

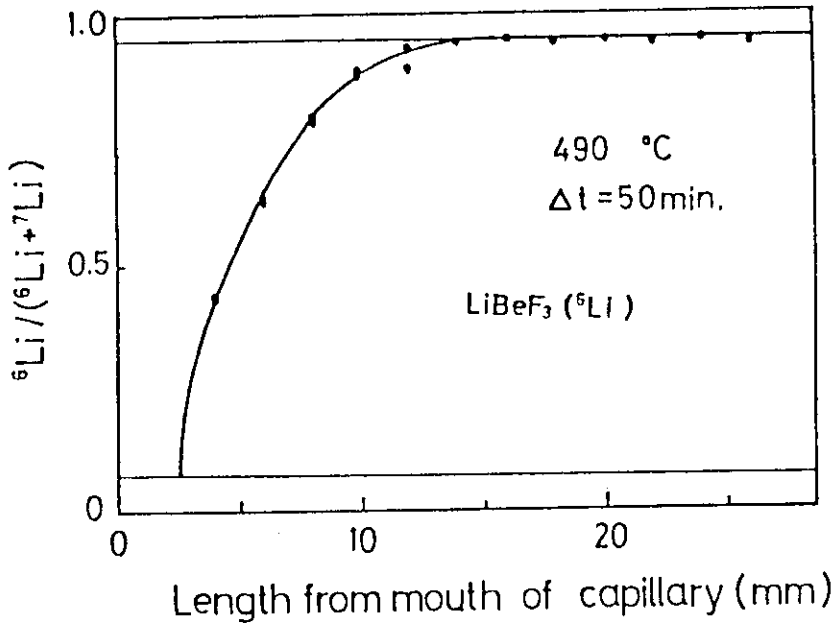

Fig.9 Distribution of ^6Li in a capillary after a diffusion run.

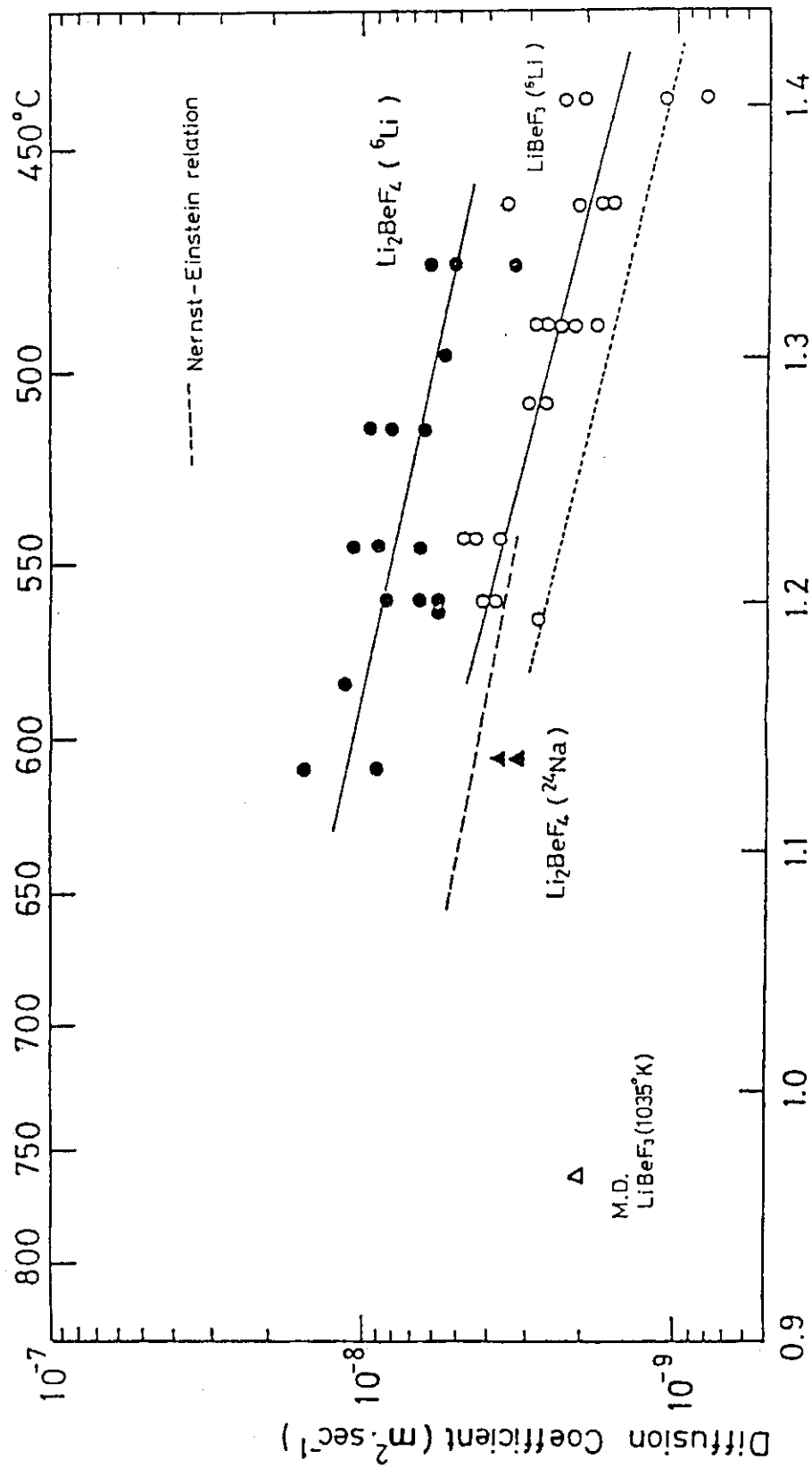

Fig.10 Self-diffusion coefficients of lithium in Li_2BeF_4(●) and $LiBeF_3$(○) melts and impurity sodium(▲) in Li_2BeF_4 melt. Open triangle shows a calculated value at 1035K by Rahman et al.[30] Dashed and dotted lines show diffusion coefficient calculated from electrical conductivities of molten Li_2BeF_4 and $LiBeF_3$, respectively.

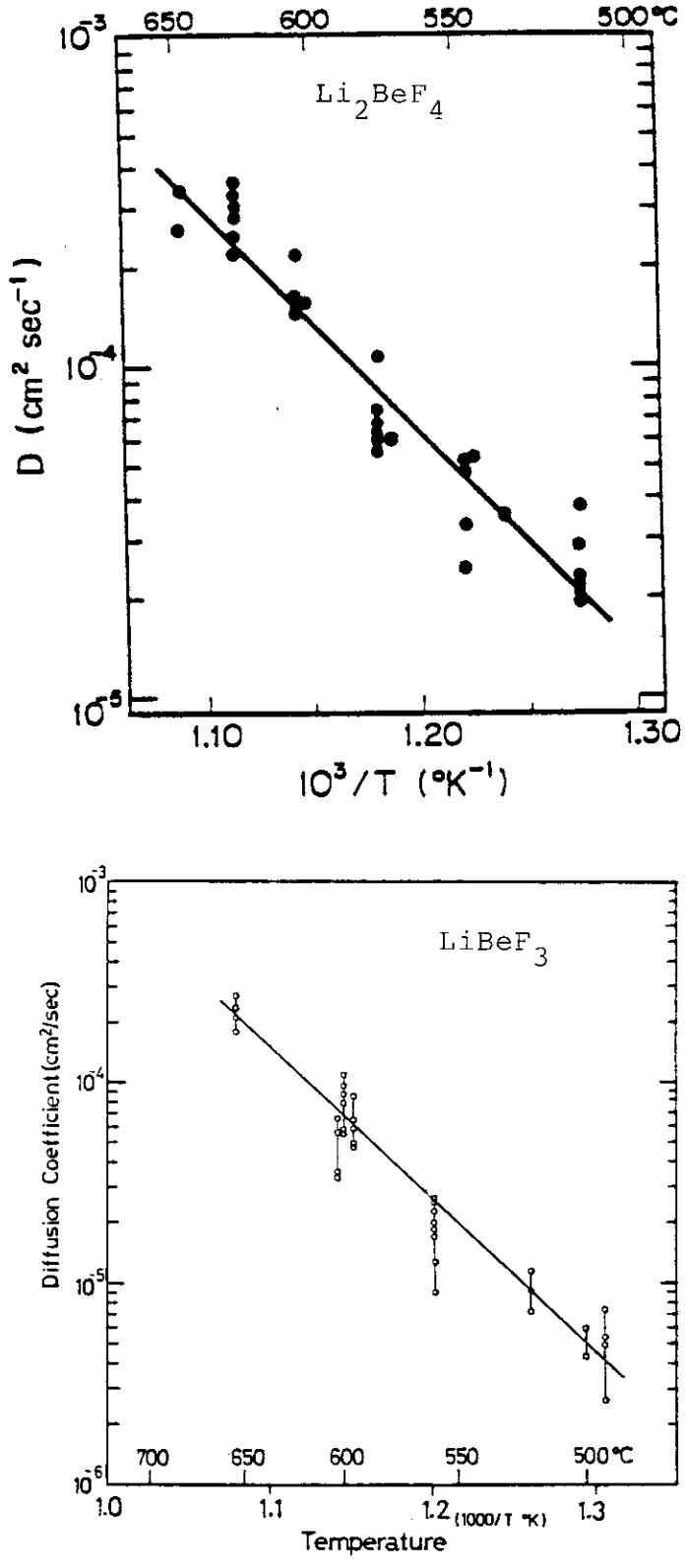

Fig.11 Self-diffusion coefficients of fluorine in Li_2BeF_3 and $LiBeF_3$ melt.

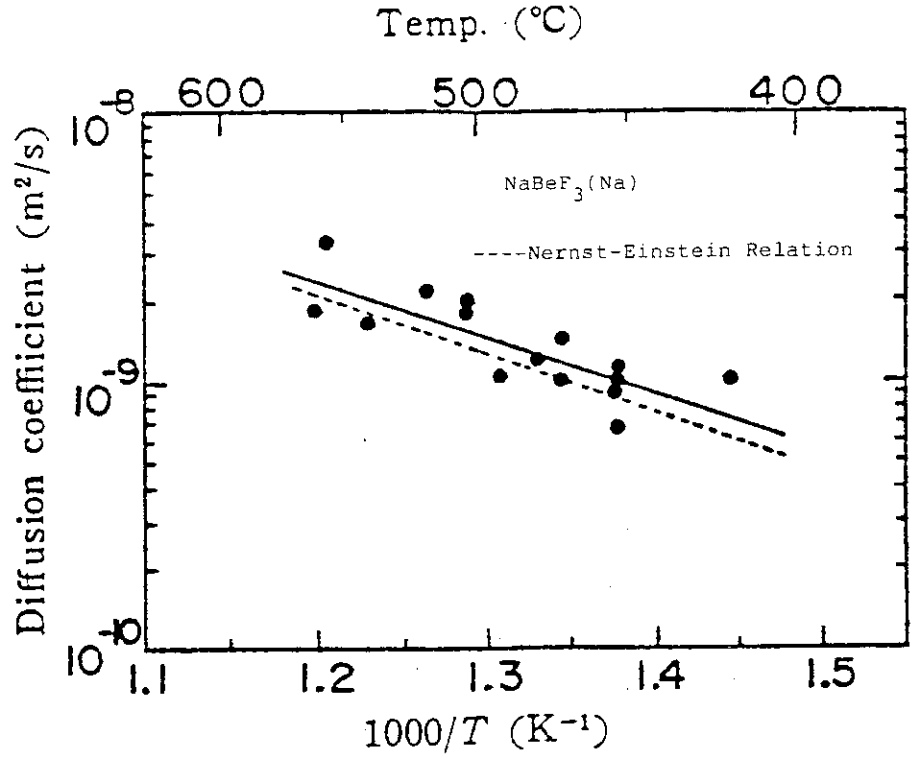

Fig.12 Self-diffusion coefficients of sodium in molten $NaBeF_3$.

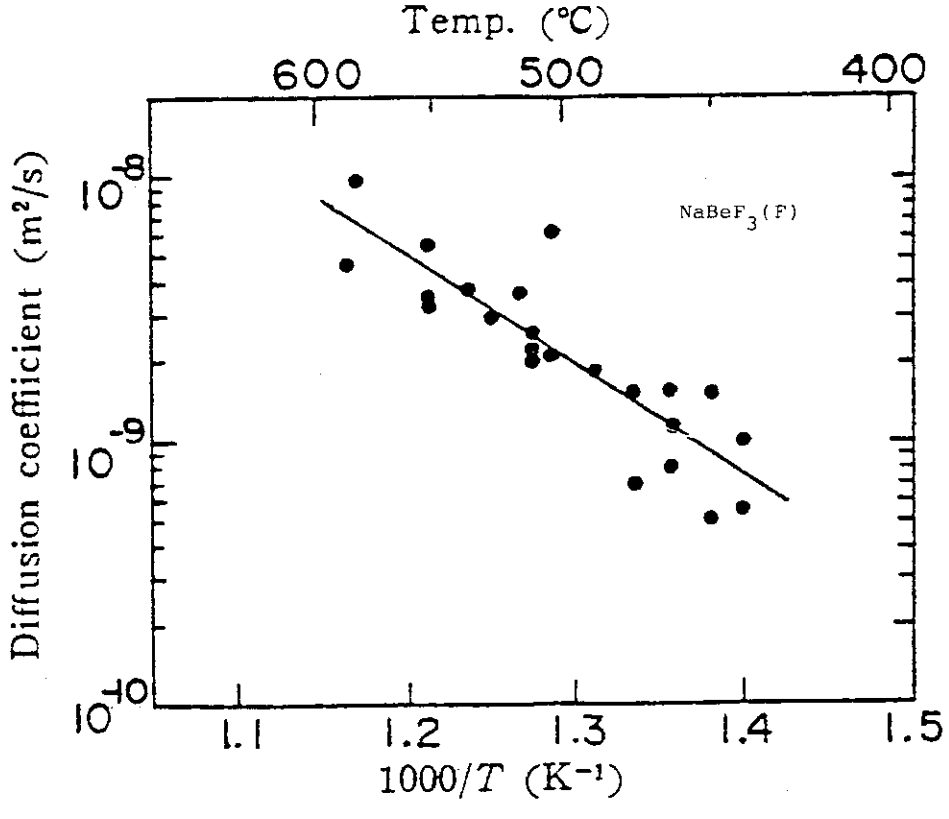

Fig.13 Self-diffusion coefficients of fluorine in molten $NaBeF_3$.

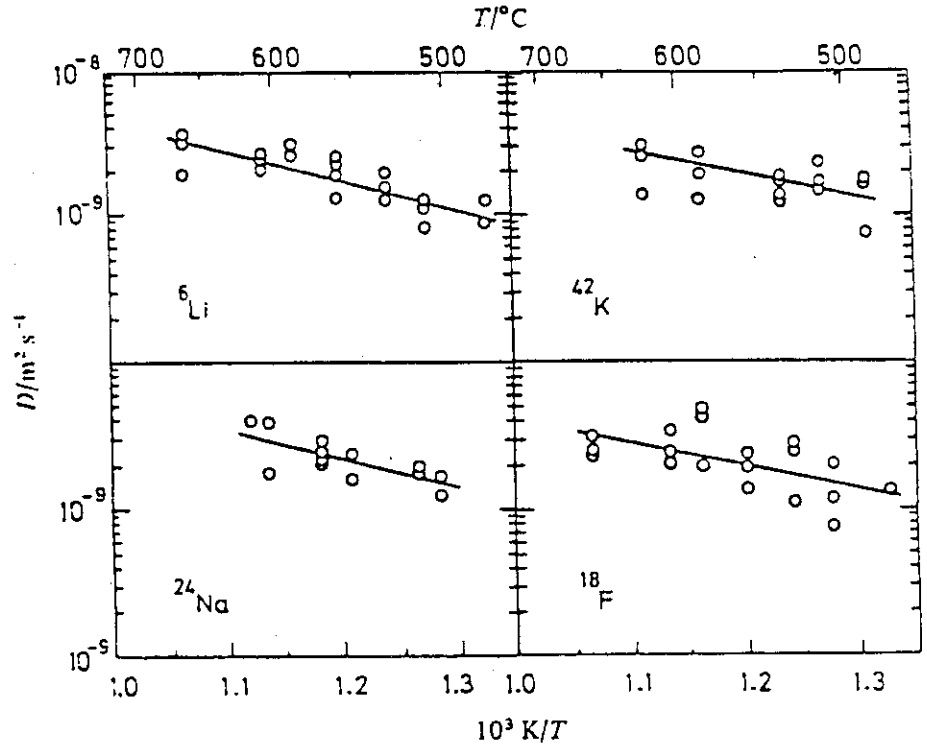

Fig.14 Self-diffusion coefficients of lithium,sodium,potassium and fluorine in molten FLINAK.

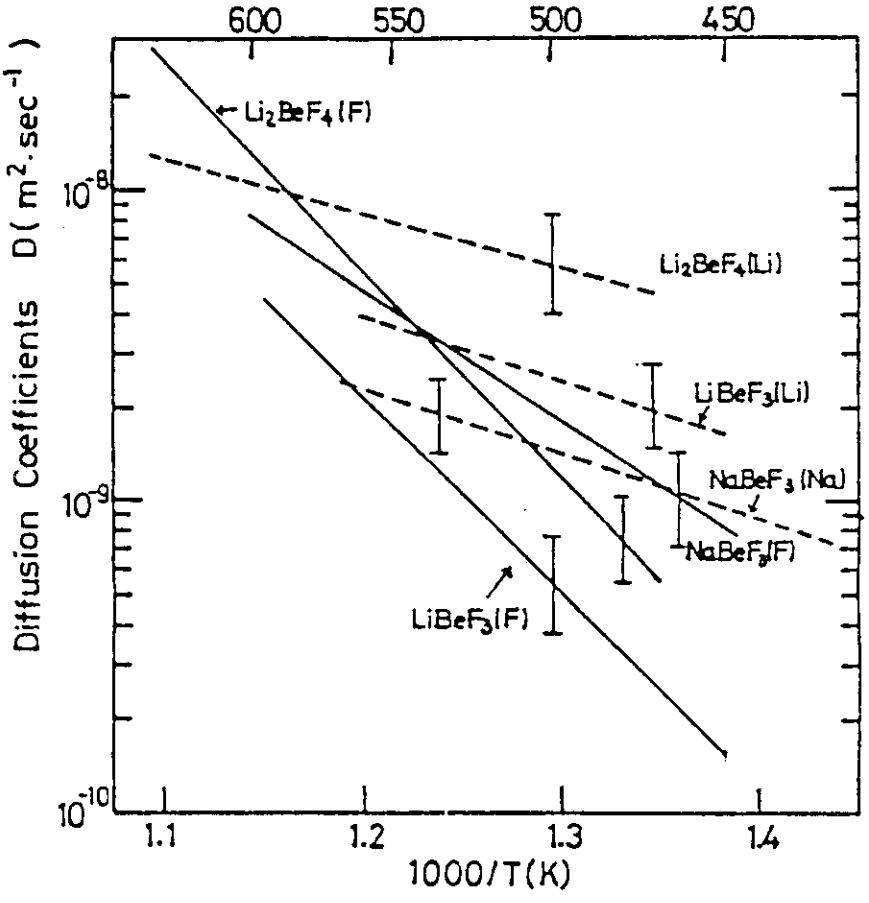

Fig.15 Summary of the self-diffusion coefficients of fluorine and lithium or sodium in molten Li_2BeF_4, $LiBeF_3$ and $NaBeF_3$.

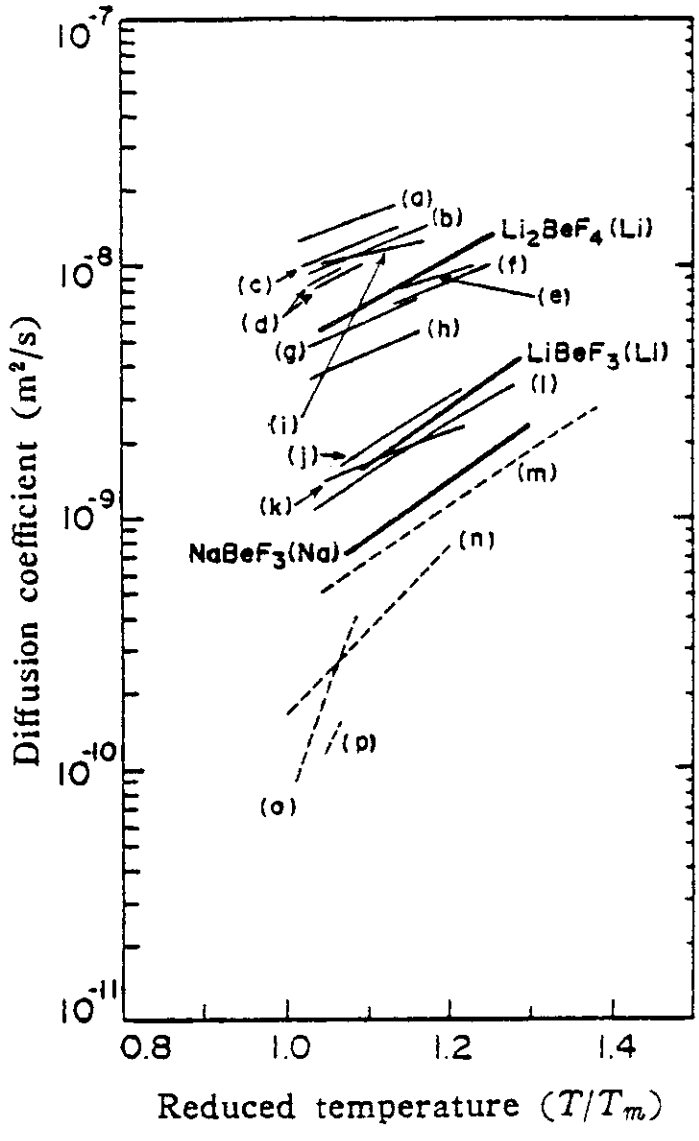

Fig.16 Comparison of self-diffusion coefficients of various cations in molten salts and molten silicates under the reduced temperature scale T/T_m.
(a)KF(K)[18];(b)NaCl(Na)[19];(c)NaF(Na)[18];(d)NaF-AlF_3(Na)[20];(e)NaI(Na)[21];(f)KCl(K)[21];(g)RbCl(Rb)[19];(h)CsCl(Cs)[19];(i)LiCl(Li)[22];(j)FLINAK(Na)[23];(k)FLINAK(K)[23];(ℓ)FLINAK(Li)[23];(m)Na_2O-SiO_2(23-77mole%)(Na)[24];(n)CaO-SiO_2-Al_2O_3(42-45-12mole%)(Ca)[25];(o)CaO-SiO_2-Al_2O_3(42-45-12mole%)(Ca)[26];(p)CaO-SiO_2(56-44 mole%)(Ca)[27].

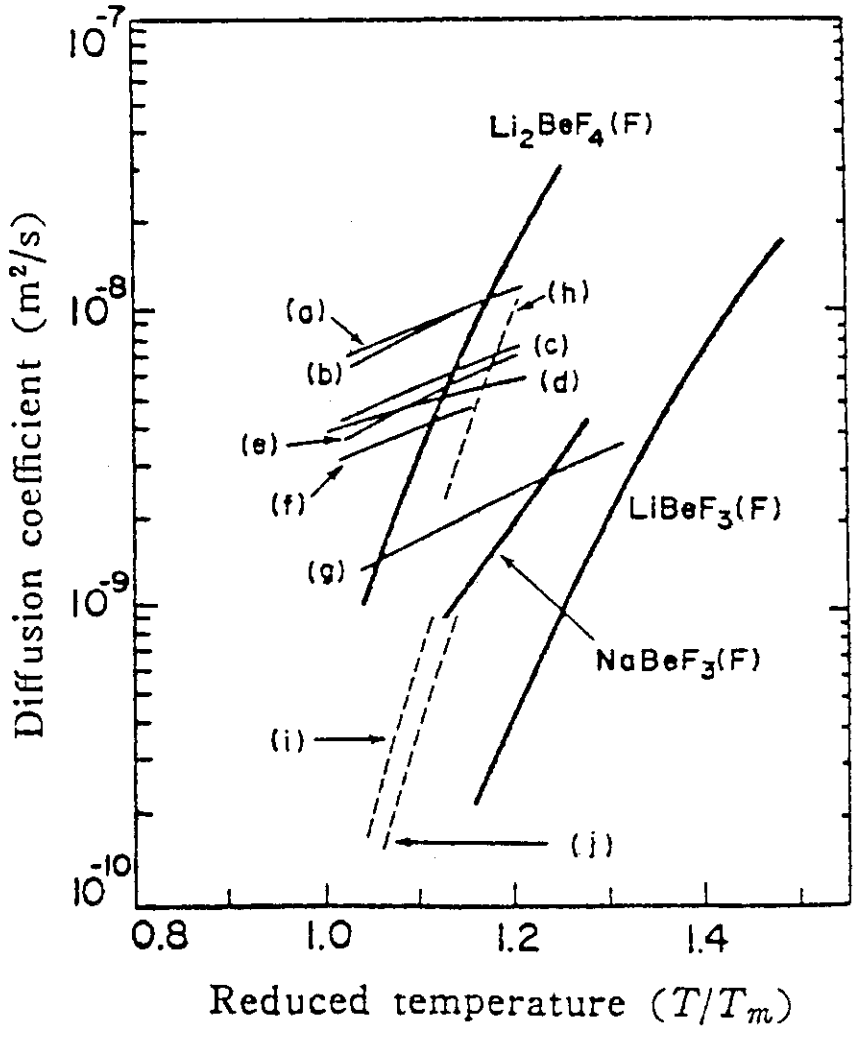

Fig.17 Self-diffusion coefficients of anions.
(a)KCl(Cl)[21];(b)NaCl(Cl)[19];(c)RbCl(Cl)[19];(d)NaI(I)[19];(e)CsCl(Cl)[19];(f)TlCl(Cl)[28];(g)FLINAK(F)[23];(h)CaO-SiO_2(56-44mole%)(O)[29];(i)CaO-SiO_2-Al_2O_3(42-45-12mole%)(O)[16];(j)CaO-SiO_2(40-60mole%)(O)[15].

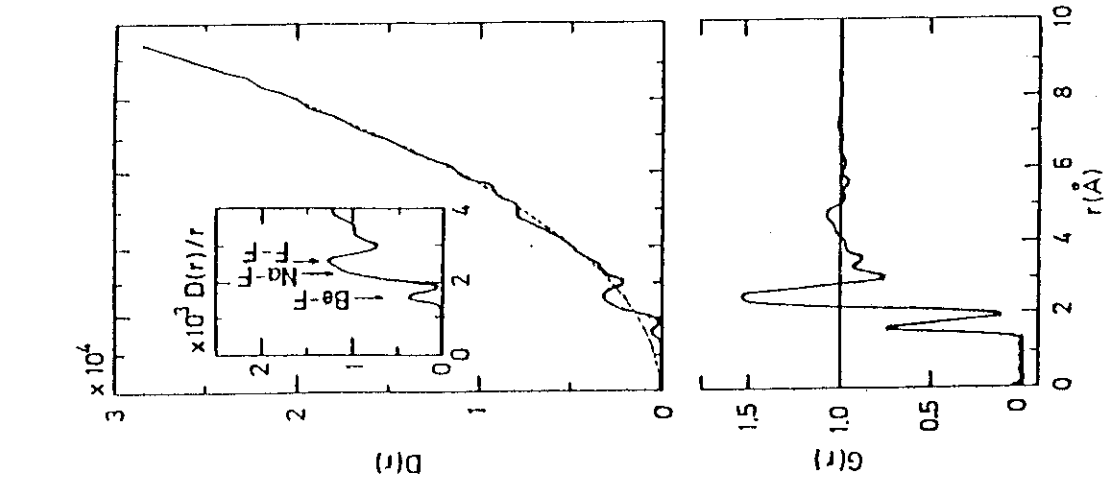

Fig.19 Radial distribution function of molten $NaBeF_3$ at 470°C.

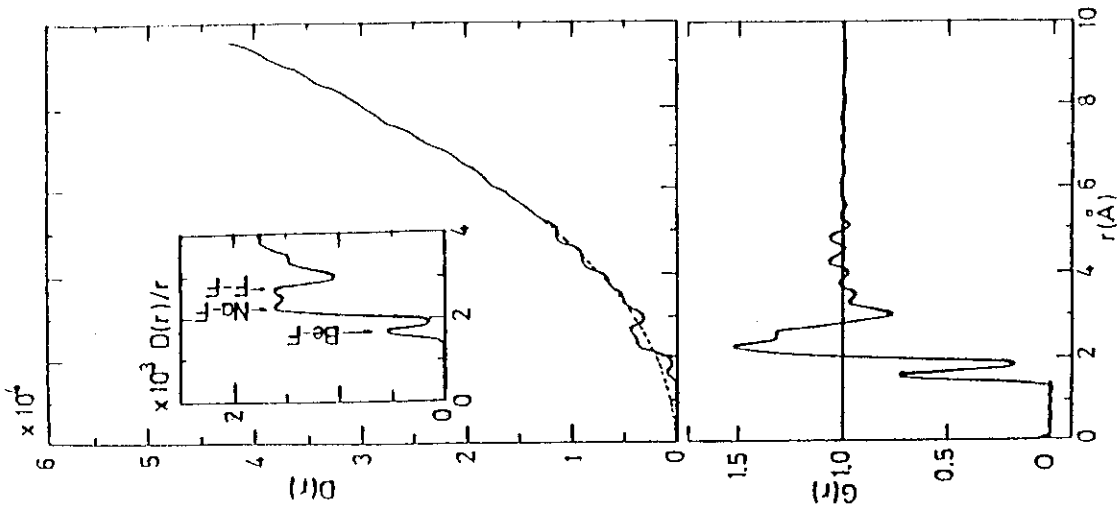

Fig.18 Radial distribution function of molten Na_2BeF_4 at 650°C.

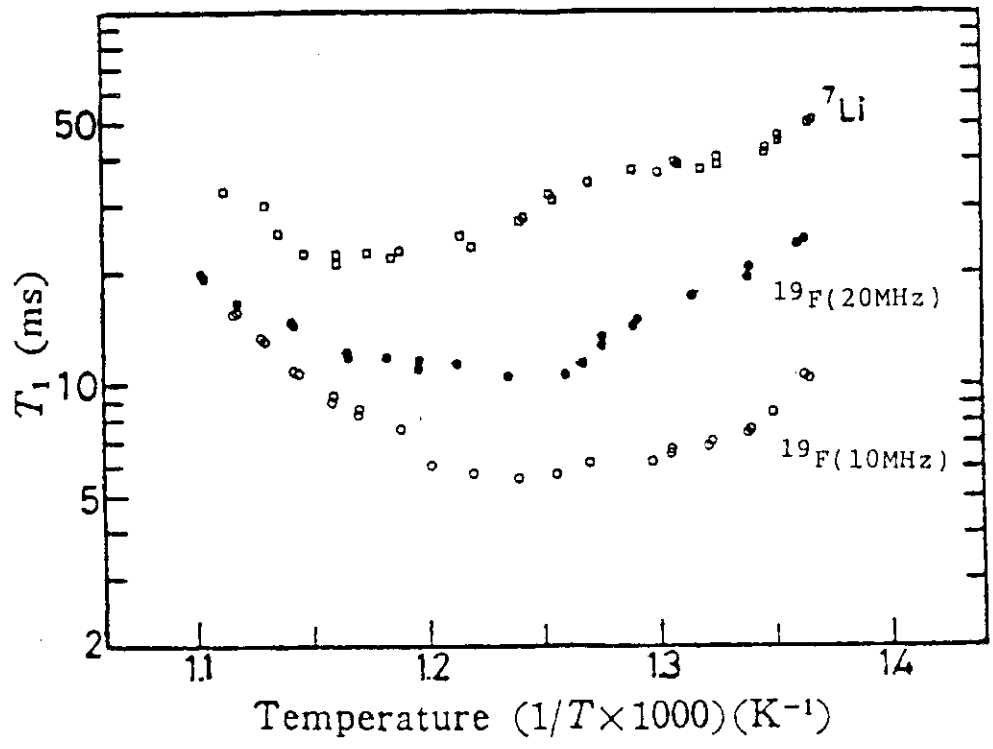

Fig.20 Temperature dependence of T_1 of ^{7}Li and ^{19}F in molten Li_2BeF_4.

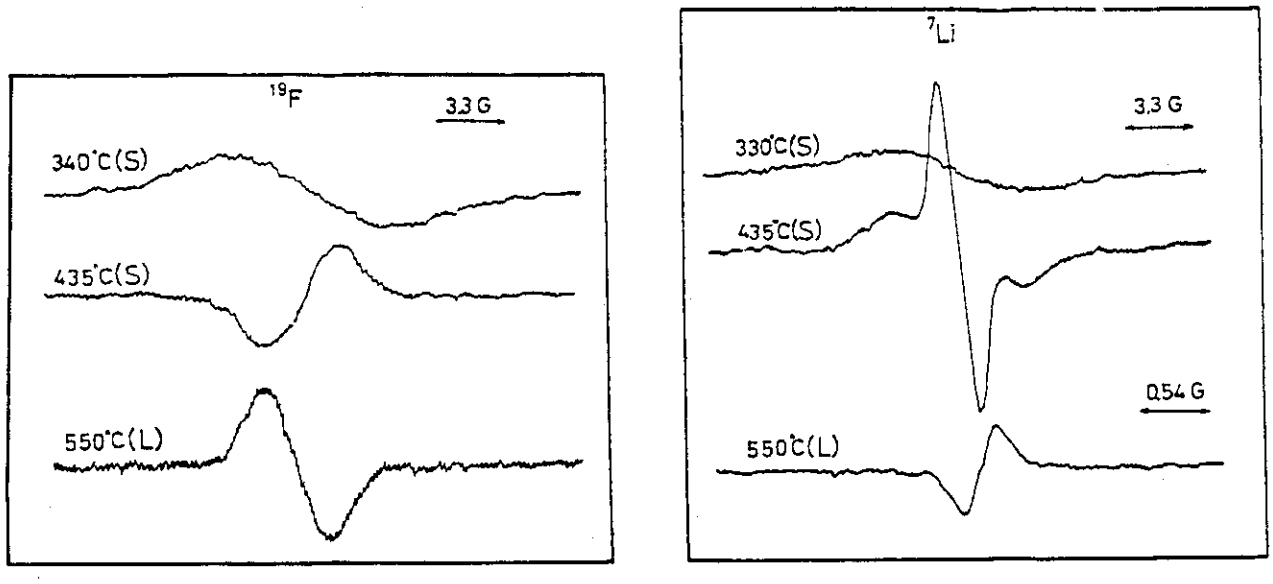

Fig.21 Resonance absorption spectra of ^{19}F and ^{7}Li.

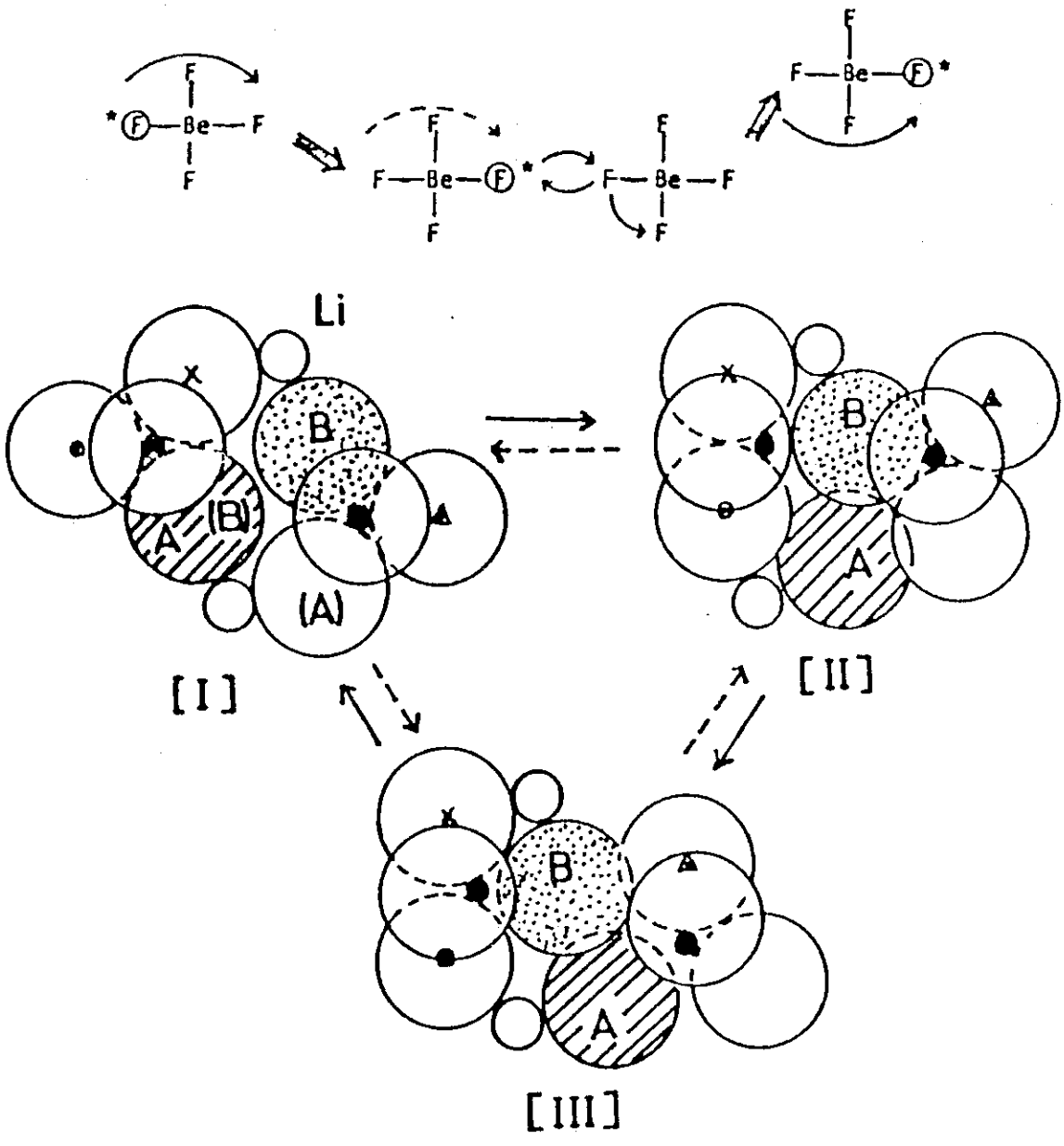

Fig.22 Rotation and exchange mechanism of self-diffusion of fluorine in molten alkali fluoroberyllates.

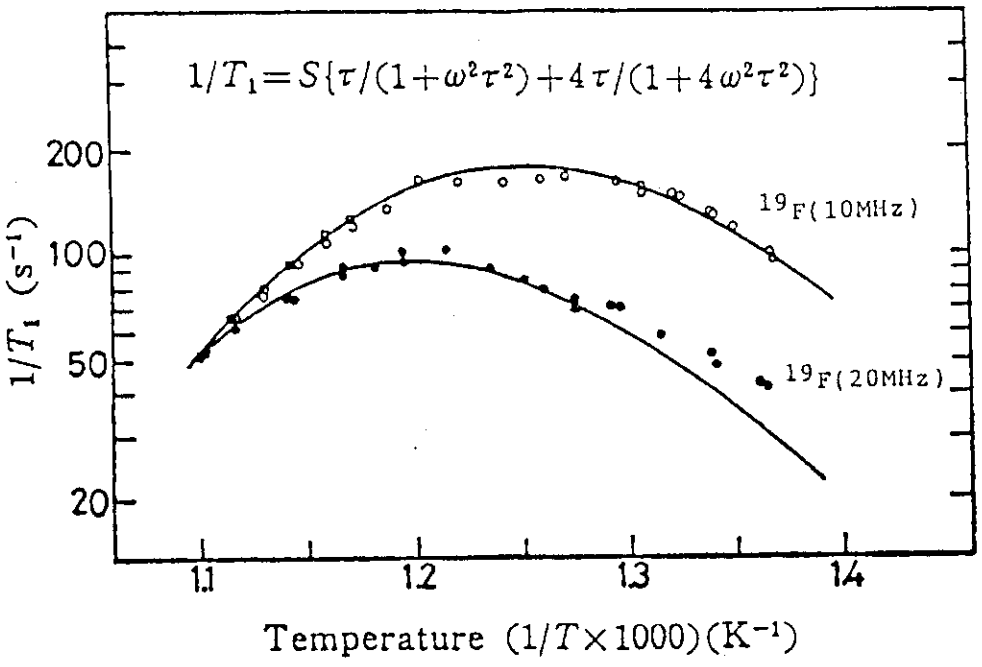

Fig.23 Temperature dependence of $(1/T_1)$ of ^{19}F in molten Li_2BeF_4. The solid curves are the theoretical one with $1/\tau = 2\times10^{15}$ exp(-103.7/RT).

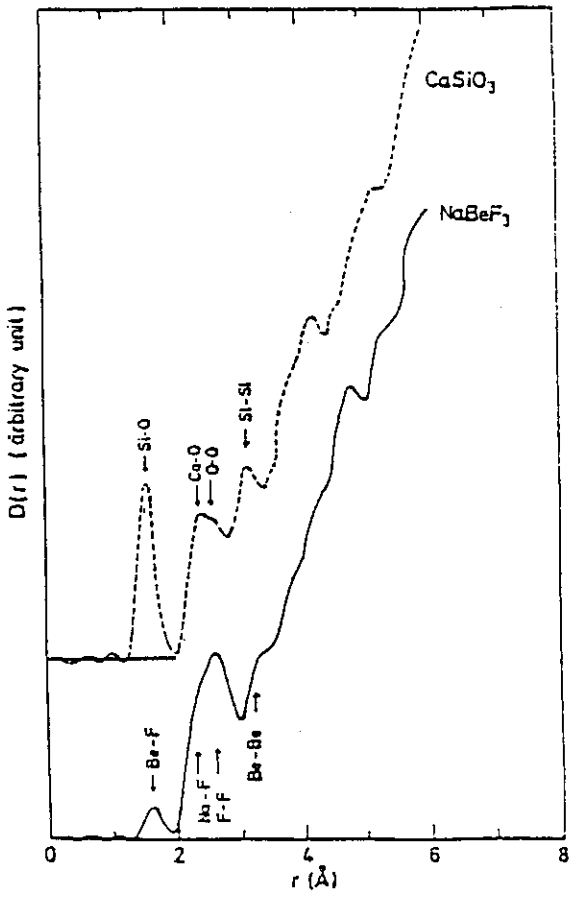

Fig.24 Comparison of radial distribution function of molten $NaBeF_3$[9] with that of molten $CaSiO_3$[17].